7 Summary and conclusions

The ability of the High-resolution Global Environmental Model (HiGEM) to simulate Queensland's rainfall, its natural variability and the drivers of that variability in a 150-year control simulation has been assessed. HiGEM displays a mean-state dry bias over tropical northern Australia and along the eastern coast (Fig. 1c) largely due to deficient rainfall in summer wet season (Fig. 1f); mean rainfall across Australia in the summer wet seasons is well simulated. The presence in HiGEM of considerable DJF wet biases just offshore, combined with the onshore dry biases, suggests that the HIGEM coastal tilting scheme permits ascent and precipitation too far away from the coastline, drying the flow before it can reach land. Aside from northern and eastern Queensland in the summer, HiGEM produces a realistic simulation of seasonal-mean Queensland rainfall.

HiGEM produces near-observed levels of inter-annual variability in rainfall across Australia, for both annual and seasonal rainfall, with slightly strong (weak) variability in northern and eastern (southern and western) Queensland (Fig. 3). The ENSO-Queensland rainfall teleconnection is robust in HiGEM in all seasons, including the seasonal variations in the strength of the correlation (i.e., highest in SON, weakest in MAM) and the spatial pattern of the correlation magnitude (Fig. 5).

The only discrepancies between HiGEM and observations are minor: correlations in northern Australia during the MAM ENSO transition season are weaker than observed, while those in DJF and JJA for eastern Australia are too strong. HiGEM produces reasonable lead–lag relationships between Niño 4 SST anomalies and Queensland rainfall (Fig. 6), except for in February and March when the overly bi-annual nature of ENSO in HiGEM leads to erroneous anti-correlations between rainfall in those months and the ENSO in the remainder of the same calendar year. The observed asymmetric response of Queensland rainfall to Niño 4 SST anomalies—in which the magnitude of rainfall anomalies is correlated with the amplitude of La Niña, but not with the amplitude of El Niño—occurs in HiGEM as well, although the correlation with La Niña is overly dependent upon two large La Niña events in HiGEM that are outside the range of observed events (Fig. 7). HiGEM therefore represents well the inter-annual variations in Queensland's rainfall and its teleconnection with ENSO, the dominant driver of such variability.

On decadal temporal scales, however, HiGEM produces very weak variations in Australian rainfall, relative to the SILO analyses (Fig. 4). This is hypothesised to be due to the lack of an Interdecadal Pacific Oscillation in HiGEM, which in observations has been shown to vary both the total rainfall in Queensland and the strength of the ENSO–Queensland rainfall teleconnection (e.g. Cai et al. 2001; Arblaster et al. 2002; Power et al. 2006; Cai et al. 2010). Despite using a variety of techniques to isolate the IPO in HiGEM—EOFs of 13-year lowpass-filtered SSTs (as in Arblaster et al. 2002), regressions of global 13-year lowpass-filtered SSTs onto 13-year lowpass-filtered SSTs in the equatorial Pacific, and wavelet transforms—little coherent variability between tropical and extra-tropical Pacific SSTs on decadal temporal scales was identified (Fig. 8).

Analysis of the 1000-year control simulation (in 150 year segments) from an older, lower-resolution version of the Hadley Centre coupled model (HadCM3) discovered IPO-like features, demonstrating that such SST variability can exist in a coupled GCM. An extension of the HiGEM control simulation is planned, which would allow a longer period to be discarded from the start of the simulation to account for ocean spin-up. HiGEM lacks natural decadal variability in Queensland rainfall, likely due to the failure of the model to simulate an IPO that resembles observations.

The climatology of tropical-cyclone activity near Queensland in HiGEM compares reasonably well with observations in cyclone tracks and genesis and lysis regions (Fig. 9): there are too many cyclones in HiGEM tracking north of Australia and through the central Pacific, with slightly too few near the east coast of Queensland south of Cairns (Fig. 9c). HiGEM generates most of its cyclones near the Gulf of Carpentaria, consistent with observations (Fig. 9f); differences in lysis density are due to the inclusion of extra-tropical transitions in the HiGEM tracks but not in the observed ones (Fig. 9i). The fidelity of tropical-cyclone variability in HiGEM on all temporal scales (i.e. sub-seasonal to inter-decadal) and the links to known drivers (e.g. ENSO and the Madden–Julian Oscillation) is an active area of research in this project that will be reported separately.

Empirical orthogonal teleconnection analysis of seasonal HiGEM precipitation in Queensland revealed that the model produces many patterns of coherent rainfall variability that are similar to those from SILO, both in their spatial patterns and their underlying physical mechanisms. Table 2 summarises the region each EOT affects, the most likely driving mechanism for each EOT and the SILO EOT to which each HiGEM EOT corresponds, if any.

As in observations (Figs. 26a–d), the leading HiGEM EOTs (Figs. 11a–d) are uni-polar across Queensland and so describe state-wide rainfall variations. In DJF, JJA and SON, these patterns are highly correlated with Niño 4 SST anomalies (Table 1) and associated shifts in tropical circulation patterns, driving cyclonic circulation anomalies and increased cyclonic activity over northern Australia in wet years (Fig. 14), as Klingaman (2012b) found for the SILO EOTs. HiGEM produces weaker variance in Niño 4 SSTs associated with these EOTs, however, than in observations, and the SST anomalies do not peak strongly in DJF (Fig. 15). The leading MAM EOT in HiGEM is related to the strength of the late-season monsoon circulation across Australia, as for SILO, but the anomalous circulation in HiGEM is much weaker than in observations for similar changes in Queensland rainfall (Fig. 17).

Once the leading HiGEM EOTs were removed, the remaining EOTs describe patterns of coherent regional rainfall variations in Queensland. As for the leading patterns, many of these strongly resemble EOTs of SILO rainfall, although the HiGEM EOTs often do not occur in the same order (e.g. HiGEM DJF EOT 2 is similar to SILO DJF EOT 3) due to slight differences in the percentage of variance in the all-Queensland rainfall that each EOT explains. HiGEM performed particularly well for DJF EOTs, despite its mean-state dry bias in this season, which is encouraging the majoritys of Queensland's rainfall occurs during DJF, particularly in the north. HiGEM DJF EOTs 2 and 4 match SILO EOTs 3 and 2, respectively: the former is driven by onshore moisture transport from the combination of low pressure off the coast of Queensland and high pressure in the Tasman Sea (Figs. 18); the latter is caused by variations in tropical-cyclone tracks across the Cape York peninsula (Fig. 16).

By contrast, HiGEM performed poorly for SON EOTs, as only the leading SON EOT has a SILO counterpart. The other HiGEM EOTs were either driven by the same mechanism as in observations but affected the wrong region of Queensland (SON EOT 3) or affected the same region but by the wrong mechanism (SON EOT 2). In MAM and JJA, the leading two HiGEM EOTs matched the leading two SILO EOTs, with the second EOTs being driven by coastal cyclones and Southern Ocean blocking, respectively. Consistent with the overall lack of decadal variability in HiGEM, the EOTs that showed consistent decadal and multi-decadal variability in SILO have little such variability in HiGEM (Fig. 13).

The HiGEM control integration simulates well the mean and inter-annual variability of Queensland's rainfall and its drivers, even capturing the second EOT of SILO rainfall in three of four seasons. The ENSO–Queensland rainfall teleconnection is particularly robust in HiGEM, as are patterns of regional rainfall variability that involve onshore flow along the Queensland coast. Tropical cyclones are also captured well, although drivers of their variability in HiGEM require further investigation. On decadal temporal scales, however, HiGEM performs poorly, most likely due to a weak IPO. These results will inform the analysis of the HiGEM decadal hindcast and prediction simulations for CMIP5, as they indicate which aspects of Queensland's rainfall the model simulates reliably, and which it does not.

Appendix A

SILO EOTs

The spatial patterns (Fig. 27) and time series (Fig. 28) of the three leading EOTs of SILO seasonal rainfall from Klingaman (2012b) are included here for ease of comparison to the EOTs of HiGEM seasonal rainfall, as are the tables of correlations of potential drivers with the SILO EOTs (Table 3) and the summary table listing the mechanism that drives rainfall variability in each EOT (Table 4).

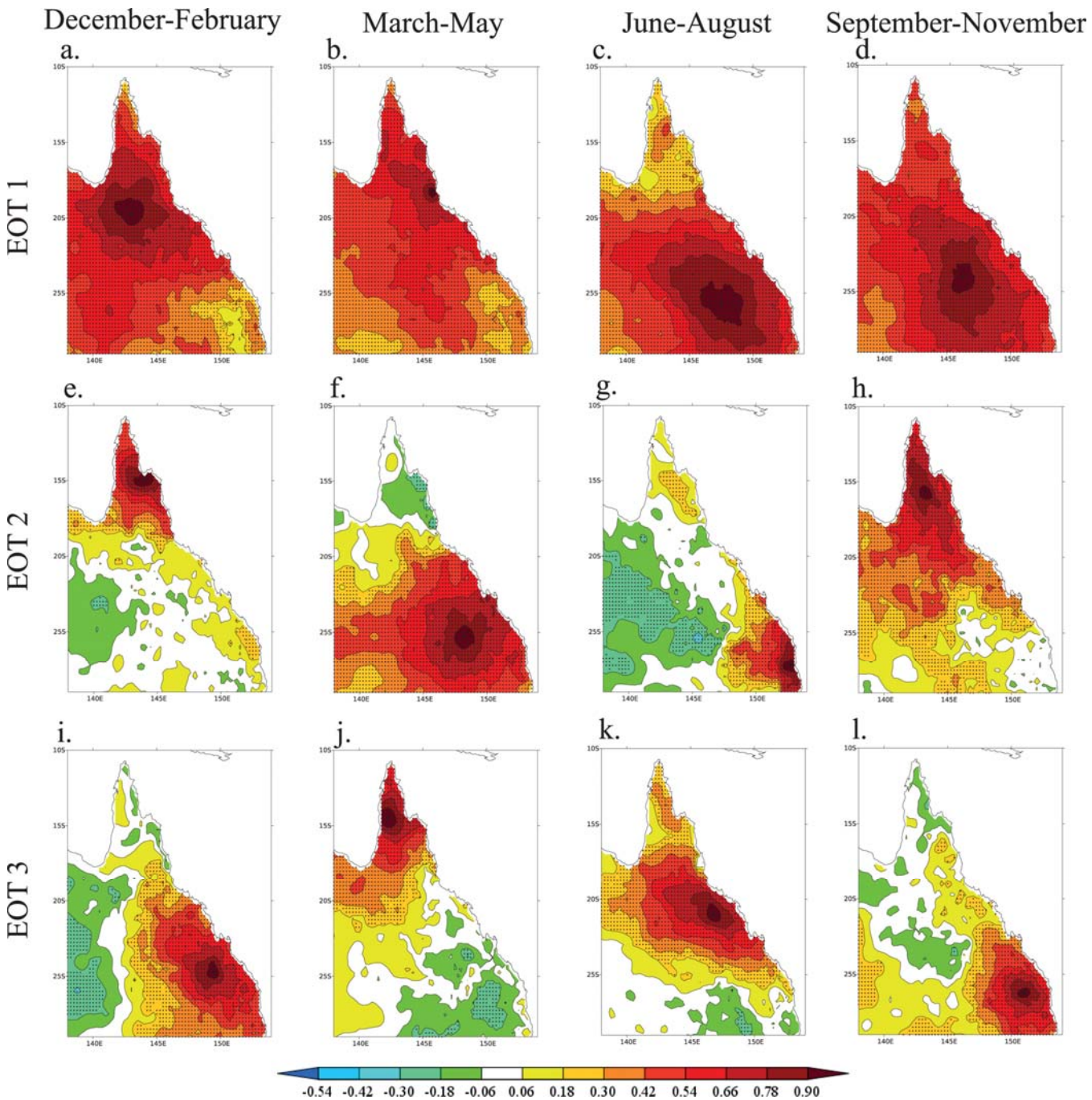

Figure 26: Correlations of the timeseries of seasonal-total (for EOT 1) or residual seasonal-total (EOTs 2 and 3) rainfall at each point with the EOT base point, which is marked with a black triangle. The base point is the one that explains the greatest

variance in the area-average (EOT 1) or the residual area-average (EOTs 2 and 3) Queensland rainfall once any preceding EOTs have been removed by linear regression. Black dots indicate statistically significant correlations at 5 per cent.

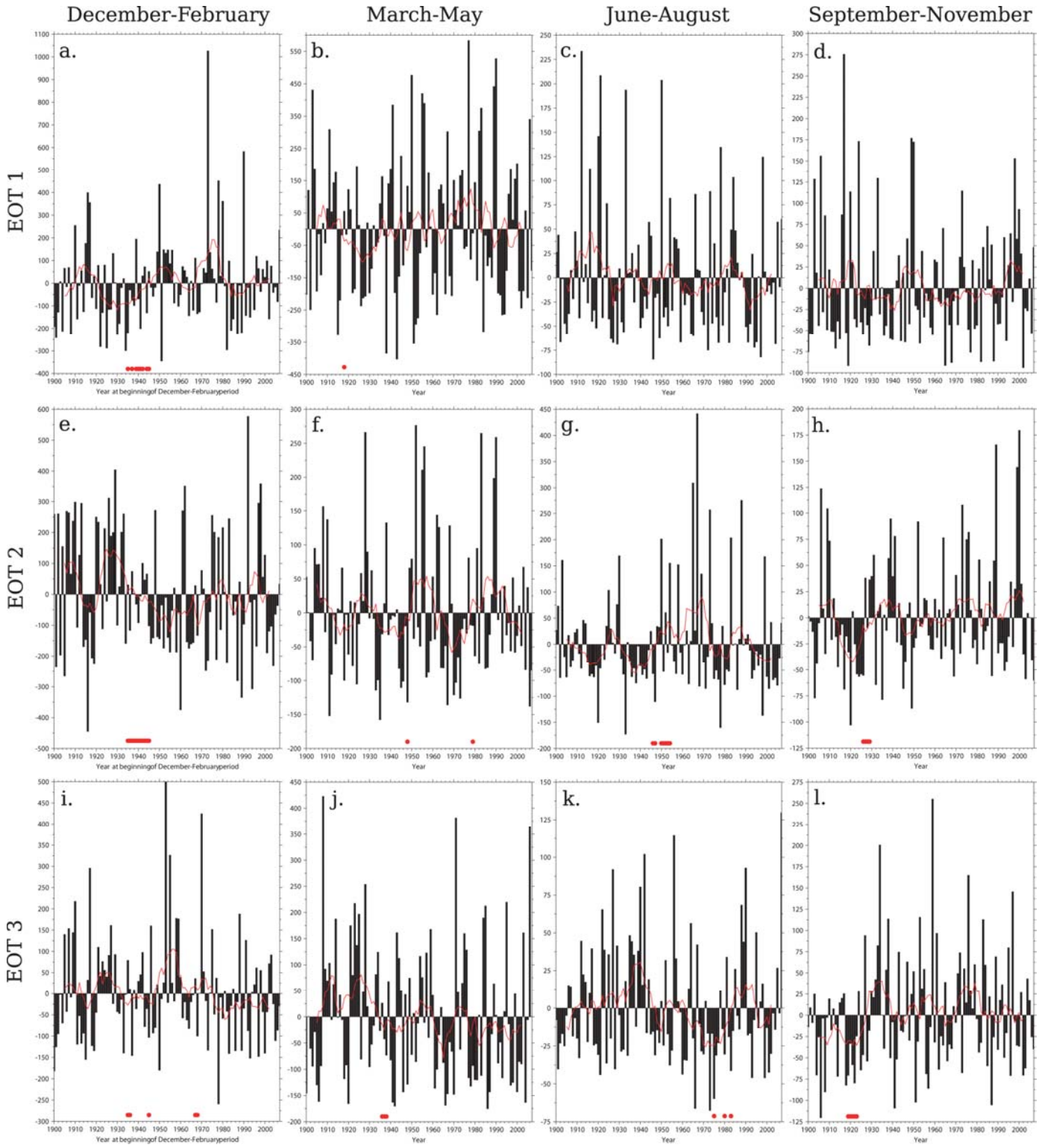

Figure 27: Annual timeseries (black bars) and their 11-year running means (red lines) for each of the EOTs in Fig. 24. Red dots near the horizontal axis indicate when the 31-year centred linear trend is statistically significant at the 5 per cent level. All time series are expressed as anomalies from their mean for ease of interpretation.

Season and EOT	Variance explained	Niño 4	IPO	$B_{120\ 150}$	$B_{150\ 180}$	SAM	$SAM_{\text{Niño 4}}$	IOD	$IOD\|_{\text{Niño 4}}$
December–February									
EOT 1	37.71%	−0.35**	−0.44**	−0.04	0.03	0.28	0.24	0.00	0.11
EOT 2	8.63%	−0.20	−0.02	−0.04	−0.10	0.15	0.12	−0.07	0.05
EOT 3	7.36%	−0.18	−0.22	0.24*	0.12	0.05	0.00	−0.19	−0.12
March–May									
EOT 1	32.17%	−0.17	−0.19	−0.02	−0.16	0.09	0.09	0.07	0.07
EOT 2	13.54%	−0.06	0.01	0.21	−0.15	−0.05	−0.04	0.10	0.10
EOT 3	8.64%	−0.39**	−0.36**	0.05	0.18	0.16	0.15	0.01	0.02
June–August									
EOT 1	45.12%	−0.37**	−0.29*	0.23	0.00	0.25	0.38*	−0.01	−0.07
EOT 2	9.85%	−0.13	−0.11	−0.10	0.26*	0.08	0.11	−0.03	−0.06
EOT 3	6.63%	−0.04	−0.08	0.11	0.19	−0.32*	−0.30*	0.05	0.05
September–November									
EOT 1	41.34%	−0.44**	−0.39**	0.29*	0.18	0.34*	0.32*	−0.25	−0.05
EOT 2	10.91%	−0.30*	−0.25*	0.09	0.12	0.00	−0.06	−0.31*	−0.09
EOT 3	6.80%	−0.12	−0.04	0.26*	0.12	0.31*	0.30*	0.09	0.10

Table 3: For the three leading EOTs of seasonal Queensland rainfall from SILO: the percentage of variance in the area-averaged, seasonal Queensland rainfall explained; the correlations between the EOT time series and Niño 4, the Interdecadal Pacific Oscillation index, the Bureau of Meteorology blocking index longitude-averaged over 120–150°E and 150–180°E, the Southern Annular Mode index and the Indian Ocean Dipole index. For the Southern Annular Mode and the Indian Ocean Dipole, partial correlations with EOT time series are also computed, removing the influence of Niño 4; these are denoted by $|_{\text{Niño 4}}$. An * (**) indicates correlations that are statistically significant at the 5 per cent (1 per cent) level.

Season and EOT	Variance explained	Region affected	Likely driving mechanism
December–February			
EOT 1	37.71%	State-wide	ENSO (peaking) effects on Australian monsoon, modulated by IPO
EOT 2	8.63%	Cape York	Tropical cyclone activity in the Coral Sea
EOT 3	7.36%	Southern	Coastal cyclones and onshore winds
March–May			
EOT 1	32.17%	State-wide	Strength of late-season monsoon, local air–sea interactions
EOT 2	13.54%	Central and southern	Extra-tropical storm track, 500 hPa convergence and moistening
EOT 3	8.64%	Northern	ENSO (decaying) effects on late-season Australian monsoon
June–August			
EOT 1	45.12%	State-wide	ENSO (developing) and SAM influences on extra-tropical storm track
EOT 2	9.85%	Southeastern and western	Blocking in Tasman Sea, driving onshore winds
EOT 3	6.63%	Northern	Coastal cyclones, southward transport of tropical moisture
September–November			
EOT 1	41.34%	State-wide	ENSO (developing) and SAM influences on extra-tropical storm track
EOT 2	10.91%	Northern	ENSO (decaying), southward transport of tropical moisture
EOT 3	6.80%	Southeastern	Unclear, but associations with SAM and Southern Ocean blocking

Table 4: Summary of EOT analysis, giving percentage of variance explained in Queensland-average rainfall, the region of Queensland encompassed by the pattern, and the likely driving mechanism for each EOT.

8 Glossary

Baroclinic - Refers to a condition and type of motion in which pressure is not constant on surfaces of constant density, e.g. internal tides and other internal waves.

Blocking anticyclone - Large scale patterns in the atmospheric pressure field that are nearly stationary, effectively "blocking" or redirecting migratory cyclones. They are also known as blocking highs or blocking anticyclones.

Climate change - A study dealing with variations in climate on many different time scales from decades to millions of years, and the possible causes of such variations. In the most general sense, the term "climate change" encompasses all forms of climatic inconstancy (that is, any differences between long-term statistics of the meteorological elements calculated for different periods but relating to the same area) regardless of their statistical nature or physical causes.

Climate variability - The inherent characteristic of climate which manifests itself in changes of climate with time. The degree of climate variability can be described by the differences between long-term statistics of meteorological elements calculated for different periods.

Cut-off lows - Areas of low surface pressure, closed circulation and intense mid-and upper-tropospheric baroclinic development that form to the south of Australia during periods of atmospheric blocking.

East-coast lows - Areas of closed circulation that form near the eastern coast of Australia south of 20°S and move parallel to the coast. They develop in regions of strong zonal SST gradients and track along the eastern coastline of Australia.

El Niño Southern Oscillation (ENSO) - An irregular oscillation of equatorial Pacific Ocean upper-ocean temperatures, which occurs due to unstable atmosphere–ocean interactions. These ocean-temperature anomalies cause variations in sea-level atmospheric pressure, termed the Southern Oscillation

General Circulation Models (GCM) - Computer models designed to help understand and simulate global and regional climate, in particular the climatic response to changing concentrations of greenhouse gases. GCMs aim to include mathematical descriptions of important physical and chemical processes governing climate, including the role of the atmosphere, land, oceans, and biological processes. The ability to simulate sub-regional climate is determined by the resolution of the model.

Indian Ocean Dipole (IOD) - The difference between sea surface temperature in the western and eastern tropical Indian Oceans. A positive IOD occurs when the western basin is warmer than average and the eastern basin is cool.

Inter-decadal Pacific Oscillation (IPO) - A low-frequency mode of variability in Pacific SSTs; in its positive phase, SSTs are warmer in the East Pacific and in the central equatorial Pacific and cooler in the subtropical and extra-tropical West Pacific in both hemispheres.

Madden-Julian Oscillation (MJO) - A tropical atmospheric phenomena, with a timescale ranging from 40 to 60 days which develops over the Indian Ocean and travels eastwards through the tropics.

Southern Annular Mode (SAM) - The north-south movement of the band of westerly winds south of Australia. SAM is positive when there is a poleward shift of the westerly wind belt and is associated with enhanced spring and summer rainfall in New South Wales and Queensland.

Southern Oscillation - Traditionally defined as normalized sea-level pressure anomalies at Tahiti minus those at Darwin; positive (negative) values correspond to La Niña (El Niño).

Synoptic - Pertaining to a general view of the whole, hence a synoptic variable is one used to describe the state of system over a wide geographical area.

Trade winds - A steady easterly surface winds found in the tropics and blowing towards the equator from the northeast in the northern hemisphere or the southeast in the southern hemisphere, especially at sea. They blow from the tropical high-pressure belts to the low-pressure zone at the equator.

Tropical cyclone - A storm system characterized by a large low-pressure centre and numerous thunderstorms that produce strong winds and heavy rain. Tropical cyclones feed on heat released when moist air rises, resulting in condensation of water vapour contained in the moist air.

Walker Circulation - The east-west movement of the trade winds across the tropical Pacific Ocean, bringing moist surface air to the west with dry air returning along the surface to the east.

9 References

Arblaster, J., G. Meehl, and A. Moore, 2002: Interdecadal modulation of Australian rainfall. Clim. Dynam., 18, 519–531.

Cai, W., P. van Rench, T. Cowan, and A. Sullivan, 2010: Asymmetry in ENSO teleconnection with regional rainfall, its multidecadal variability, and impact. J. Climate, 23, 4944–4955.

Cai, W., P. H. Whetton, and A. B. Pittock, 2001: Fluctuations of the relationship between enso and northeast Australian rainfall. Clim. Dynam., 17, 421–432.

Conkright, M. E., R. A. Locarnini, H. E. Garcia, T. D. O'Brien, T. P.Boyer, C. Stephen, and J. I.Antonov, 2002: World ocean atlas 2001: Objective analyses, data statistics and figures, CD-ROM documentation. Internal Report 17, National Oceanographic Data Centre, 17 pp.

Folland, C. K., D. E. Parker, A. Colman, and R. Washington, 1999: Large scale modes of ocean surface temperature since the late nineteenth century. Beyond El Niño: Decadal and interdecadal climate variability, A. Navarra, Ed., Springer, Berlin, 73–102.

Gordon, C., C. Cooper, C. A. Senior, H. Banks, J. M. Gregory, T.C. Johns, J.F.B. Mitchell, and R.A. Wood, 2000: The simulation of SST, sea ice extents and ocean heat transports in a version of the Hadley Centre coupled model without flux adjustments. Clim. Dynam., 16, 147–168.

Hendon, D., D. Thompson, and M. Wheeler, 2007: Australian rainfall and surface temperature variations associated with the Southern Annular Mode. J. Climate, 20, 2452–2467.

Hodges, K. I., 1996: Spherical nonparametric estimators applied to the UGAMP model integration for AMIP. Mon. Wea. Rev., 124, 2914–2932.

Hopkins, L. C. and G. J. Holland, 1997: Australian heavy-rainfall days and associated east-coast cyclones: 1958–92. J. Climate, 10, 621–635.

Jeffrey, S. J., 2001: Using spatial interpolation to construct a comprehensive archive of Australian climate data. Environ. Model. Softw., 16, 309–330.

Klingaman, N. P., 2012a: A literature survey of key rainfall drivers in Queensland, Australia: Queensland Climate Change Centre of Excellence Research Report: Rainfall in Queensland. Part 1. Department of Environment and Resource Management, Queensland Government, Brisbane, Australia. Available online at www.derm.qld.gov.au

Klingaman, N. P., 2012b: Empirical orthogonal teleconnection analysis of inter-annual variability in Queensland, Australia. Queensland Climate Change Centre of Excellence Research Report: Rainfall in Queensland. Part 3. Department of Environment and Resource Management, Queensland Government, Brisbane, Australia. Available online at www.derm.qld.gov.au

Knapp, K. R., M. C. Kruk, D. H. Levinson, H. J. Diamond, and C. J. Neumann, 2010: The international best track archive for climate stewardship (IBTrACS). Bull. Amer. Meteor. Soc., 91, 363–376.

Marshall, G., 2003: Trends in the southern annual mode from observations and reanalyses. J. Climate, 16, 4134–4143.

Murphy, B. F. and J. Ribbe, 2004: Variability of south-eastern Queensland rainfall and climate indices. Int. J. Climatol., 24, 703–721.

Nicholls, N., 1989: Sea surface temperatures and Australian winter rainfall. J. Climate, 2,965–973.

Power, S., M. Haylock, R. Colman, and X. Wang, 2006: The predictability of interdecadal changes in ENSO activity and ENSO teleconnections. J. Climate, 19, 4755–4771.

Rayner, N. A., D. E. Parker, E. B. Horton, C. K. Folland, L. V. Alexander, D. P. Rowell, E. C. Kent, and A. Kaplan, 2003: Global analyses of sea surface temperature, sea ice and night marine air temperature since the late ineteenth century. J. Geophys. Res., 108, 4407.

Ringer, M. A., G. M. Martin, C. Z. Greeves, T. J. Hinton, P. M. James, V. D. Pope, A. A. Scaife, and R. A. Stratton, 2006: The physical properties of the atmosphere in the new Hadley Centre global environmental model (HadGEM1). Part II: Aspects of variability and regional climate. J. Climate, 19, 1302–1326.

Risbey, J. S., M. J. Pook, P. C. McIntosh, M. C. Wheeler, and H. H. Hendon, 2009: On the remote drivers of rainfall variability in Australia. Mon. Wea. Rev., 137, 3233–3253.

Roberts, M. J. et al., 2009: Impact of resolution on the tropical Pacific circulation in a matrix of coupled models. J. Climate, 22, 2541–2556.

Saji, N. H., B. N. Goswami, P. N. Vinayachandran, and T. Yamagata, 1999: A dipole mode in the tropical Indian Ocean. Nature, 401, 360–363.

Shaffrey, L. et al., 2009: U.K. HiGEM: The new U.K. high-resolution global environment model—Model description and basic evaluation. J. Climate, 22, 1861–1896.

Smith, I., 2004: An assessment of recent trends in Australian rainfall. Aust. Met. Mag., 53, 163–173.

Suppiah, R., K. J. Hennessy, P. H. Whetton, K. McInnes, I. Macadam, J. Bathols, J. Ricketts, and C. M. Page, 2007: Australian climate change projections derived from simulations performed for the IPCC 4th Assessment Report. Aust. Met. Mag., 131–152.

Taylor, K. E., R. J. Stouffer, and G. A. Meehl, 2009: A summary of the CMIP5 experiment design. Available from http://cmip.llnl.gov/cmip5/docs/Taylor CMIP5 design.pdf.

Thompson, D. W. J. and J. M. Wallace, 2000: Annular modes in the extratropical circulation. Part I: Month-to-month variability. J. Climate, 13, 1018–1036.

Thorncroft, C. and K. Hodges, 2001: African easterly wave variability and its relationship to Atlantic tropical cyclone activity. J. Climate, 14, 1166–1179.

Uppala, S. M. et al., 2005: The ERA-40 re-analysis. Q. J. R. Meteorol. Soc., 131, 2961–3012.

Walsh, K. J. E. and J. Syktus, 2003: Simulations of observed interannual variability of tropical cyclone formation east of Australia. Atmos. Sci. Lett., 4, 28–40.